Sensing and Bio-Sensing Research 3 (2015) 74–78

Contents lists available at ScienceDirect

Sensing and Bio-Sensing Research

journal homepage: www.elsevier.com/locate/sbsr

# A novel sensor based on $Fe_3O_4$ nanoparticles–multiwalled carbon nanotubes composite film for determination of nitrite

Jianying Qu *, Ying Dong, Yong Wang, Huanhuan Xing

*Institute of Environmental and Analytical Sciences, College of Chemistry and Chemical Engineering, Henan University, Kaifeng, Henan 475004, PR China*

ARTICLE INFO

*Keywords:*
$Fe_3O_4$ nanoparticles
Multiwalled carbon nanotubes
Nitrite

ABSTRACT

A novel nitrite sensor was constructed via electropolymerization of L-cysteine on the multiwalled carbon nanotubes and then immobilization of cationic poly(diallyldimethylammonium chloride) coated $Fe_3O_4$ nanoparticles through electrostatic interaction at glassy carbon matrix. Under the optimized conditions, the obtained sensor exhibited good electrocatalytic activity for the oxidation of nitrite, and the peak current of nitrite increased linearly with its concentration from $7.49 \times 10^{-6}$ to $3.33 \times 10^{-3}$ mol/L ($R = 0.9998$) with the detection limit of $8.46 \times 10^{-7}$ mol/L (S/N = 3). Moreover, the sensor exhibited good sensitivity, stability and repeatability with potential applications.


## 1. Introduction

Nitrite is commonly used as an industrial salt and food additive. Thus, nitrite is widespread within environment and physiological systems. According to World Health Organization, the maximum permissible amount of nitrite ion in drinking water is 50 mg/L [1,2]. Nitrite, in high levels, can form nitrosamines by interacting with amines, which are toxic and carcinogenic substances [3]. So an accurate determination of nitrite is important to protect environmental and reduce the health risks. Many techniques have been developed for determining nitrite, such as flow injection analysis, colorimetric method, chemiluminescence, electrochemical analysis and so on [4–7].

Among them, electrochemical methods are often favored over others due to the easy operation, fast response and relatively low cost [8]. Recently, different kinds of electrochemical nitrite sensors have been fabricated based on the chemical modification of electrode [9–12].

$Fe_3O_4$ magnetic nanoparticles (NPs), a half-metallic metal oxide with the inverse spinel structure [13], possess appealing magnetic properties, nontoxicity, easy synthesis and electrocatalytic capability. From the references, nitrite sensors based on $Fe_3O_4$ NPs have been reported with excellent electrocatalytic performance toward nitrite oxidation [14–16].

However, pure magnetic nanoparticles are very likely to aggregate and sensitive to oxidation for their large ratio of surface area to volume and high chemical reactivities, resulting in poor dispersibility and limiting their application to some extent [17]. Among extensive applications in magnetic resonance imaging, drug delivery, catalyst and biosensor [18–21], surface modification of $Fe_3O_4$ NPs is an important step because it prevents the $Fe_3O_4$ NPs from aggregating, improves NPs stability in suspension and enhances biocompatibility of NPs [22]. Thus, numerous coating materials, such as Pt [14], Au [16], polypyrrole [17], polydopamine [23] and citrate [24] were used to modify the surface of $Fe_3O_4$ NPs. Satisfactorily, polymer coating has good biocompatibility, stability, and provides a useful platform for further functionalization. As reported by Cheng et al. [25], $Fe_3O_4$ NPs were functionalized with cationic poly(diallyldimethylammonium chloride) (PDDA) and applied to colorimetric sensing of glucose and selective extraction of thiol, developing a new way for the synthesis of bifunctional NPs.

In this paper, positively charged PDDA coated $Fe_3O_4$ NPs (PDDA–$Fe_3O_4$) were prepared successfully by coprecipitation method. Based on this, a novel sensor was constructed through immobilization PDDA–$Fe_3O_4$ on miltiwalled carbon nanotubes (MWCNTs) film modified with L-cysteine at glassy carbon (GC) matrix. The proposed composite film combined the high surface-to-volume ratio of MWCNTs, the electrocatalytic activity of L-cys and PDDA–$Fe_3O_4$ NPs, their synergistic effect was contributed to excellent electrocatalytic performance for the oxidation of nitrite. Compared with other related reports, the proposed nitrite sensor showed high sensitivity, wide linear range, low detection limit, good stability and repeatability.

* Corresponding author. Tel.: +86 0371 3881589.
*E-mail addresses:* QJY405407@163.com, qujy@henu.edu.cn (J. Qu).

http://dx.doi.org/10.1016/j.sbsr.2014.10.009

## 2. Experimental

### 2.1. Instruments and reagents

Electrochemical measurements were performed using a CHI650 electrochemical workstation (CHI, USA) with a conventional three-electrode system, which was constituted with a GC electrode as working electrode, a platinum wire as counter electrode and a Ag/AgCl (saturated KCl) as reference electrode. The morphological characterization of the synthesized PDDA–$Fe_3O_4$ NPs were examined using X-ray diffraction (D8 Advance, Bruker) and transmission electron micrograph (JEM-100CX II, Japan).

MWCNTs (Diameter 10–15 nm, University of Marburg, Germany, Department of Chemistry, Materials Science Center); poly(diallyldimethylammonium chloride) solution (PDDA) (Sigma–Aldrich); L-cysteine (L-cys) (Tianjin Guangfu Chemical Reagent Co.); $NaNO_2$ (Tianjin Deen Chemical Reagent Co.); $FeCl_3{\cdot}6H_2O$ and $FeSO_4{\cdot}7H_2O$ (Shanghai No. 1 Reagent Factory); 28% ammonia aqueous solution. Other reagents were of analytical reagent grade. All solutions were prepared with doubly distilled water.

### 2.2. Synthesis of PDDA–$Fe_3O_4$ NPs

According to the reference [25], a modified method was used to synthesize cationic PDDA coated $Fe_3O_4$ NPs. A solution (100 mL) containing 2.7031 g $FeCl_3{\cdot}6H_2O$, 1.3901 g $FeSO_4{\cdot}7H_2O$ and PDDA (v/v, 1.0%) was deoxygenated by stirred vigorously with nitrogen gas for 20 min, followed by heating to 80 °C. Then 28% ammonia aqueous solution (10 mL) was added dropwise into the heated solution. The solution was cooled to room temperature after reaction at 80 °C for 1 h. The precipitate was collected through centrifugation, washed several times with doubly distilled water, and dried under vacuum at 65 °C for 7 h to obtain the products.

### 2.3. Preparation of the sensor

A GC electrode was polished with 1.0, 0.3, and 0.05 μm $Al_2O_3$ slurry in turn and sonicated in 1/1 nitric acid, ethanol and doubly distilled water for 3 min, respectively, dried at room temperature for use.

8 μL 1.15 mg/mL DMF-dispersed MWCNTs suspension was casted on the GC electrode surface and dried it under the infrared lamp to get a MWCNTs/GC electrode.

The electropolymerization of L-cys on the MWCNTs/GC electrode was carried out by cyclic scanning in the potential range of 2.5 V to −1.0 V for 5 cycles in 0.1 mol/L PBS (pH 6.0) with 5 mmol/L L-cys using a scan rate of 100 mV/s. The resulting L-cys/MWCNTs/GC electrode was rinsed with doubly distilled water to remove the physical adsorbed L-cys and dried at room temperature. Then the L-cys/MWCNTs/GC electrode was immersed in the positively charged PDDA–$Fe_3O_4$ NPs aqueous dispersion for 1 h to fabricate the PDDA–$Fe_3O_4$/L-cys/MWCNTs/GC electrode.

## 3. Results and discussions

### 3.1. Characterization of $Fe_3O_4$ NPs and PDDA–$Fe_3O_4$ NPs

As shown in the Fig. 1, the XRD patterns of the $Fe_3O_4$ NPs (a) and PDDA–$Fe_3O_4$ NPs (b) were examined. From the figure, the diffraction peaks at $2\theta$ angles of about 30.5°, 35.5°, 43.0°, 53.8°, 57.0° and 62.7°, which could be indexed to (220), (311), (400), (422), (511) and (440) planes of the face-centered cubic lattice of $Fe_3O_4$, respectively. These characteristic peaks of the PDDA–$Fe_3O_4$ NPs were consistent with those of the $Fe_3O_4$ NPs, reflecting that

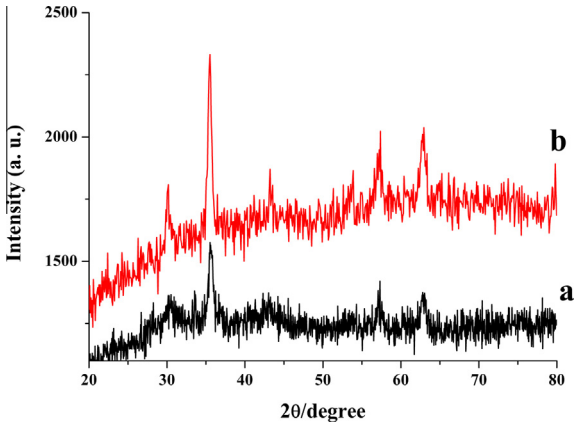


**Fig. 1.** XRD patterns of the prepared $Fe_3O_4$ NPs (a) and PDDA–$Fe_3O_4$ NPs (b).

adding PDDA to a precursor solution did not perturb the formation of the $Fe_3O_4$ NPs.

Fig. 2 displayed the TEM images of $Fe_3O_4$ NPs (A) and PDDA–$Fe_3O_4$ NPs (B). The $Fe_3O_4$ NPs were nanosized and the average size was approximate 10–15 nm with uniform distribution. After being coated with PDDA, the average diameter of PDDA–$Fe_3O_4$ NPs was about 20–25 nm.

### 3.2. Optimization of experimental parameters

#### 3.2.1. Effect of WMCNTs dispersion amount

The effect of the modification amount of MWCNTs on the response peak current of 0.5 mmol/L nitrite was investigated. As shown in Fig. 3, the response peak current of nitrite enhanced gradually with increasing volume of MWCNTs from 2 to 8 μL, then almost did not increase from 8 to 10 μL. When further increasing the modification amount, the peak current showed a decreasing tendency. This might because that excessive thickness of the film would hinder the electron transfer on the sensor surface. So, the optimum amount of MWCNTs was 8 μL.

#### 3.2.2. Effect of L-cys electropolymerization cycles

Cyclic voltammetry was used to form the polymer film with different cycles. Inset of Fig. 4 showed that L-cys (PBS, pH 6.0) was electrochemically polymerized on the surface of MWCNTs/GC electrode successfully. Fig. 4 demonstrated that the response current increased with the increasing of polymerization cycles from 0 to 5 and then decreased tendency when the polymerization cycles was more than 5. So, 5 cycles of electrochemical polymerization was selected as the optimum condition.

#### 3.3.2. Influence of pH

The influence of the solution pH on the peak current was studied from 4.0 to 8.0. As shown in Fig. 5, the peak current increased with the increasing of pH up to 5.5 and decreased at higher pHs. The peak current reached a maximum at pH 5.5. At pH values lower than 5.5, the lower current might be caused by the protonation of nitrite ions. At pH values higher than 5.5, the lower current might because that the oxidation of nitrite was inhibited by oxide layers on the electrode surface. Therefore, pH 5.5 was used for further studies.

### 3.4. Electrocatalytic oxidation of nitrite at different electrodes

Cyclic voltammetry was applied to investigate the electrochemical behaviors of 0.5 mmol/L nitrite at bare GC, MWCNTs/GC, L-cys/MWCNTs/GC and PDDA–$Fe_3O_4$/L-cys/MWCNTs/GC electrodes in

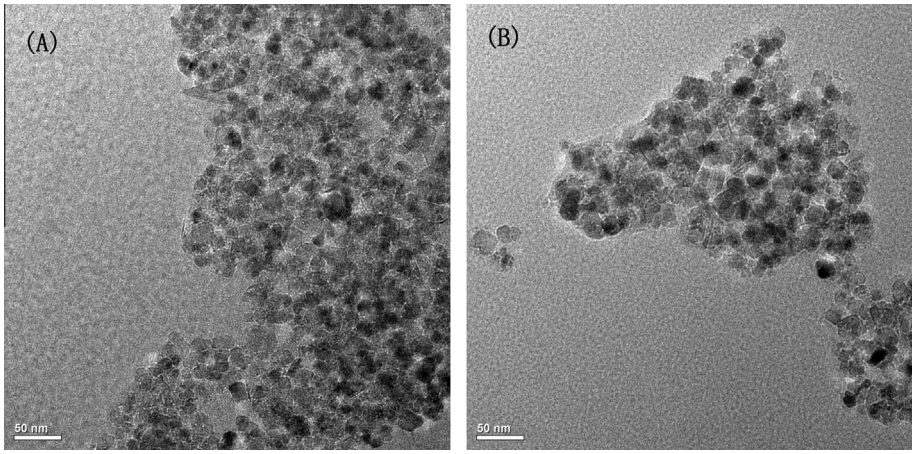


**Fig. 2.** TEM images of the prepared $Fe_3O_4$ NPs (A) and PDDA–$Fe_3O_4$ NPs (B).

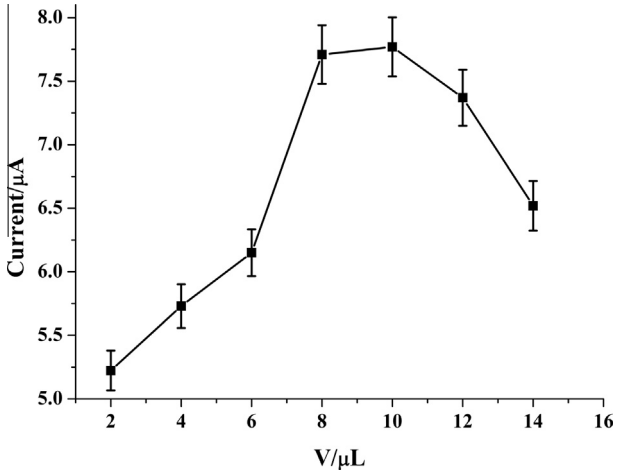


**Fig. 3.** Influence of MWCNTs amount on the peak current of nitrite.

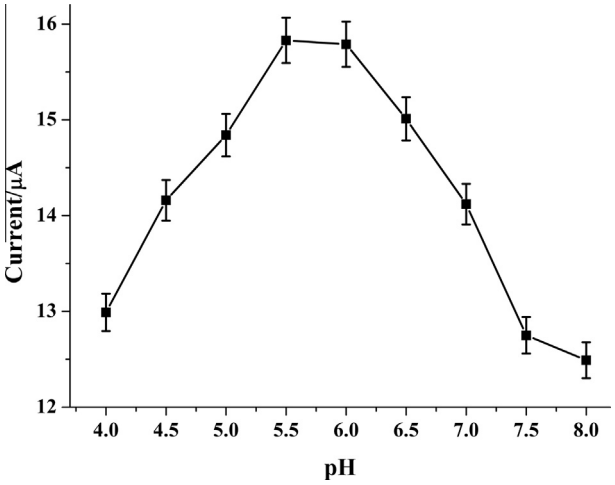


**Fig. 5.** Influence of pH on the peak current of 0.5 mmol/L nitrite in 0.1 mol/L PBS.

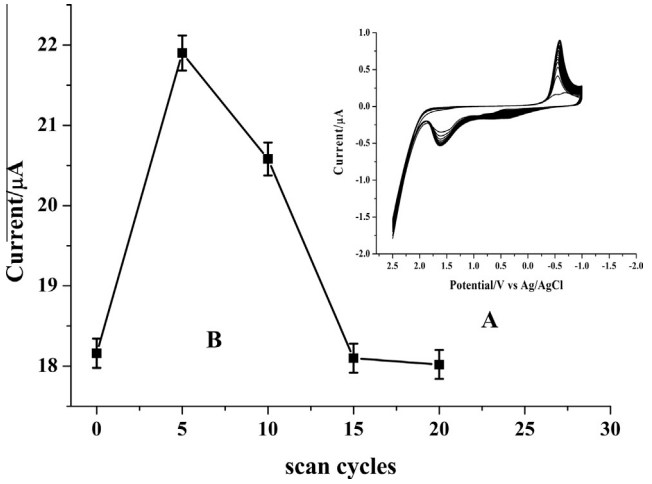


**Fig. 4.** Influence of L-cys electropolymerization cycles on the peak current of 0.5 mmol/L nitrite in 0.1 mol/L PBS; Inset: Electropolymerization of 5 mmol/L L-cys at MWCNTs/GC electrode in 0.1 mol/L PBS (pH 6.0) using a scan rate of 100 mV/s.

0.1 mol/L PBS (pH 5.5). As shown in Fig. 6(A), only a small and wide peak was observed at bare GC electrode (curve a). Compared with bare GC electrode, the oxidation peak enlarged at the MWCNTs/GC electrode (curve b) and the potential shifted negatively. The surface area was enlarged by the three-dimentional porous structure of MWCNTs, which was conducive to diffusion and adsorption of nitrite to the electrode surface, but the MWCNTs/GC electrode exhibited large charging current. A more obvious increase of oxidation current and decrease of overpotential could be observed at L-cys/MWCNTs/GC electrode (curve c), indicating L-cys had good electrocatalytic activity for the oxidation of nitrite. Furthermore, PDDA–$Fe_3O_4$/L-cys/MWCNTs/GC electrode (curve d) presented a well-defined oxidation peak, largest response current and the most negative peak potential.

Moreover, cyclic voltammograms of nitrite at PDDA–$Fe_3O_4$/L-cys/MWCNTs/GC electrode in the absence (curve e) and presence (curve f) of 0.5 mmol/L nitrite were obtained and shown in Fig. 6(B). Clearly, no electrochemical signal was seen in curve e, an obvious and specific signal peak occurred in curve f, indicating that the nitrite sensor based on PDDA–$Fe_3O_4$/L-cys/MWCNTs composite film possessed excellent electrocatalytic property for the oxidation of nitrite. Therefore, the synergetic function of MWCNTs, L-cys and PDDA–$Fe_3O_4$ was contributed to the enhancement of the oxidation peak current of nitrite at the prepared sensor.

### 3.5. Effect of scan rate

Scan rate could influence the response current of nitrite. Fig. 7 showed cyclic voltammogram of the sensor at various scan rates

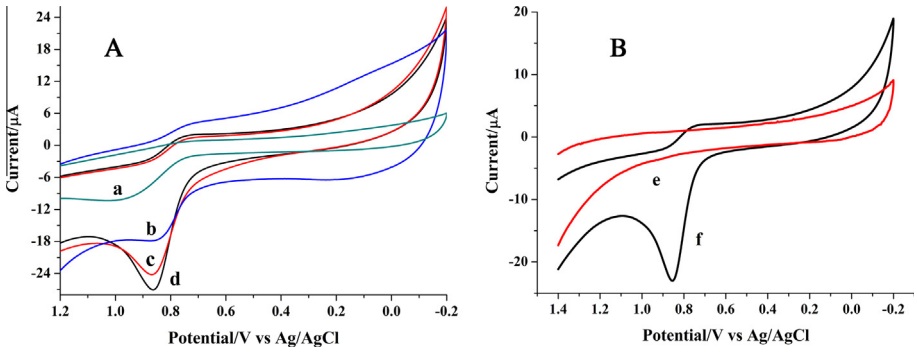


**Fig. 6.** (A) CVs of bare GC (a), MWCNTs/GC (b), L-cys/MWCNTs/GC (c), and PDDA–$Fe_3O_4$/L-cys/MWCNTs/GC (d) electrodes in 0.1 mol/L PBS (pH 5.5) containing 0.5 mmol/L nitrite; (B) CVs of PDDA–$Fe_3O_4$/L-cys/MWCNTs/GC electrode in 0.1 mol/L PBS (pH 5.5) with the absence (e), and presence (f) of 0.5 mmol/L nitrite.

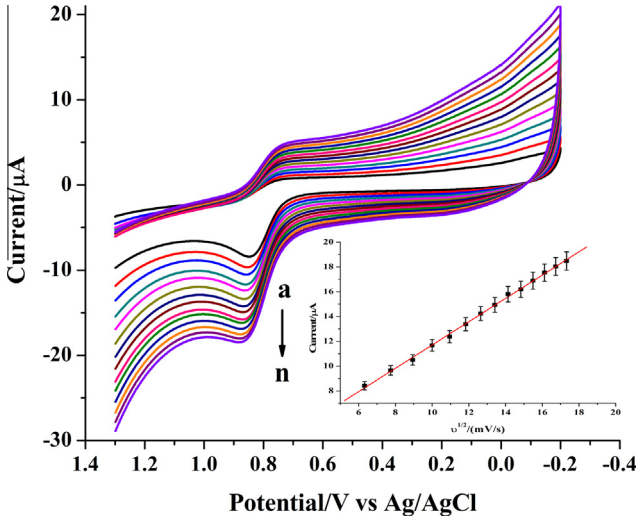


**Fig. 7.** (A) CVs of PDDA–$Fe_3O_4$/L-cys/MWCNTs/GC electrode in 0.1 mol/L PBS (pH 5.5) containing 0.5 mmol/L nitrite at different scan rates (from a to n: 40, 60, 80, 100, 120, 140, 160, 180, 200, 220, 240, 260, 280, 300 mV/s); (B) Plots of the dependence of the peak current on the scan rates.

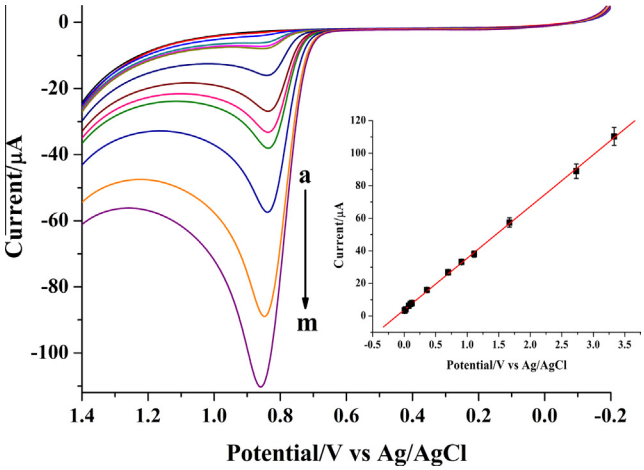


**Fig. 8.** Electrochemical response curves at the PDDA–$Fe_3O_4$/L-cys/MWCNTs/GC electrode in 0.1 mol/L PBS (pH 5.5) with different concentrations of nitrite (from a to m: 0, 0.00749, 0.0249, 0.0744, 0.099, 0.123, 0.361, 0.698, 0.909, 1.11, 1.67, 2.73, 3.33 mmol/L); Inset: Plots of peak currents vs. [$NO_2^-$].

in 0.1 mol/L PBS of pH 5.5 containing 0.5 mmol/L nitrite. Inset of Fig. 7 indicated the oxidation peak currents increased linearly with the square root of scan rates in the range of 40–300 mV/s, which was described by the following equation: $I_p$ (μA) = 2.309 + 0.9392 $\upsilon^{1/2}$ (mV/s) ($R$ = 0.9993), suggesting that the process of nitrite oxidation was controlled by diffusion.

### 3.6. Analytical characteristics

Under the optimized conditions, electrochemical response curves at the PDDA–$Fe_3O_4$/L-cys/MWCNTs/GC electrode were obtained in 0.1 mol/L PBS (pH 5.5) containing different concentrations of $NaNO_2$ and shown in Fig. 8. Obviously, the oxidation peak currents increased gradually with the increasing concentration of $NaNO_2$. Inset of Fig. 8 represented the calibration curve for the determination of $NaNO_2$. Linear dependency could be observed between the current response and concentration of nitrite in the range of $7.49 \times 10^{-6}$–$3.33 \times 10^{-3}$ mol/L, the linear regression equation was $I_p$ (μA) = 3.857 + 31.71C (mmol/L) with a correlation coefficient of 0.9998. Furthermore, a low detection limit of $8.46 \times 10^{-7}$ mol/L nitrite was determined at the signal-to-noise ratio of 3.

As could be seen from Table 1, these results were comparable or better than nitrite detection with other related sensors, such as wider linear range or lower detection limit.

**Table 1**
Comparison of other related modified electrodes for the determination of nitrite with the prepared sensor.

| Refs. | Modified electrode | Linear range (mol/L) | Detection limit (mol/L) |
|---|---|---|---|
| [9] | L-cys/GC | $1.0 \times 10^{-6}$–$4.4 \times 10^{-5}$ | $1.0 \times 10^{-7}$ |
| [10] | Pd-Fe/GC | $6.0 \times 10^{-6}$–$5.0 \times 10^{-3}$ | $2.0 \times 10^{-6}$ |
| [11] | Au/MA/GC | $1.0 \times 10^{-5}$–$1.0 \times 10^{-3}$ | $8.9 \times 10^{-7}$ |
| [12] | Cyt c/L-cys/Au | $5.0 \times 10^{-6}$–$4.5 \times 10^{-4}$ | $1.5 \times 10^{-7}$ |
| [15] | {Hb/$Fe_3O_4$@Pt}n/CS/GC | $1.5 \times 10^{-6}$–$1.2 \times 10^{-4}$ | $2.9 \times 10^{-7}$ |
| This work | PDDA–$Fe_3O_4$/L-cys/MWCNTs/GC | $7.49 \times 10^{-6}$–$3.33 \times 10^{-3}$ | $8.46 \times 10^{-7}$ |

### 3.7. Stability and repeatability

Stability and repeatability were two key factors to evaluate nitrite sensor performance based on PDDA–$Fe_3O_4$/L-cys/MWCNTs composite film. For detection of 0.5 mmol/L nitrite, the response current remained nearly 94.7% of its initial value after successive scanned for 20 cycles. And the relative standard deviation (RSD) for 7 successive determinations was about 1.4%. Thus, the proposed method had good stability and repeatability for nitrite determination.

**Table 2**
Results of the recovery experiment.

| Added (mmol/L) | Measured value (mmol/L) | Recovery (%) | Average recovery (%) |
|---|---|---|---|
| 0.361 | 0.357 | 98.9 | 101.4 |
| 0.698 | 0.686 | 98.3 | |
| 0.909 | 0.976 | 107.4 | |
| 1.67 | 1.74 | 104.2 | |
| 2.73 | 2.68 | 98.2 | |

### 3.8. Interferences

Possible interferences for the detection of nitrite at the PDDA–$Fe_3O_4$/L-cys/MWCNTs/GC electrode were investigated by adding various species into the PBS (pH 5.5) containing 0.5 mmol/L nitrite. The results indicated that common ions, such as $NH_4^+$, $Na^+$, $K^+$, $Ca^{2+}$, $NO_3^-$, $SO_4^{2-}$ and $CH_3COO^-$ had no interference on nitrite determination by the proposed electrode even when they were present in 100-fold excess over nitrite. Other potential organic interferences had also been examined. It was found that 50-fold citric acid, glucose and sodium citrate also had no significant interference for the detection of 0.5 mmol/L nitrite, indicating that the developed sensor possessed high selectivity for determination of nitrite.

### 3.9. Applications

The proposed PDDA–$Fe_3O_4$/L-cys/MWCNTs/GC electrode was applied to detect the concentration of nitrite under the optimized conditions. Standard addition method was adopted to estimate the accuracy. The determined concentrations and calculated recoveries were listed in Table 2. Clearly, the results were satisfactory with the recovery in the range of 98.2–107.4%. This indicated that the prepared sensor was reliable for the detection of nitrite.

## 4. Conclusions

In this paper, PDDA coated $Fe_3O_4$ NPs were prepared by the coprecipitation method. PDDA–$Fe_3O_4$/L-cys/MWCNTs/GC modified electrode was constructed via electropolymerization and electrostatic interaction. Cyclic voltammetry was applied to investigate the performance of nitrite on the sensor. Combined the advantages of PDDA–$Fe_3O_4$, L-cys and MWCNTs, the prepared sensor showed good electrocatalytic activity for nitrite oxidation and displayed wide linear range, low detection limit, good stability and selectivity, which showed a wide prospect for potential applications.

## Conflict of interest

The authors declare that they have no conflict of interest.

## Acknowledgments

This work was supported by the Education Department of Henan Province (No. 13A150077).

## References

[1] W.Q. Yue, D.Y. Zheng, C.G. Hu, S.S. Hu, Fabrication and application of Poly(alizarin red S)-carbon nanotubes composite film based nitrite sensor, J. Nanosci. Nanotechnol. 10 (2010) 6586–6593.
[2] P. Muthukumar, S.A. John, Gold nanoparticles decorated on cobalt porphyrin-modified glassy carbon electrode for the sensitive determination of nitrite ion, J. Colloid Interface Sci. 421 (2014) 78–84.
[3] S.S. Mirvish, Role of N-nitroso compounds (NOC) and N-nitrosation in etiology of gastric, esophageal, nasopharyngeal and bladder cancer and contribution to cancer of known exposures to NOC, Cancer Lett. 93 (1995) 17–48.
[4] M. Yaqoob, B.F. Biot, A. Nabi, P.J. Worsfold, Determination of nitrate and nitrite in freshwaters using flow-injection with luminal chemiluminescence detection, Luminescence 27 (2012) 419–425.
[5] H.J. Zhang, S.D. Qi, Y.L. Dong, X.J. Chen, Y.Y. Xu, Y.H. Ma, X.G. Chen, A sensitive colorimetric method for the determination of nitrite in water supplies, meat and dairy products using ionic liquid-modified methyl red as a colour reagent, Food Chem. 151 (2014) 429–434.
[6] L.L. Liu, Q. Ma, Z.P. Liu, Y. Li, X.G. Su, Detection of trace nitrite in waters using a QDs-based chemiluminescence analysis system, Anal. Bioanal. Chem. 406 (2014) 879–886.
[7] S. Radhakrishnan, K. Krishnamoorthy, C. Sekar, J. Wilson, S.J. Kim, A highly sensitive electrochemical sensor for nitrite detection based on $Fe_2O_3$ nanoparticles decorated reduced grapheme oxide nanosheets, Appl. Catal., B 148 (2014) 22–28.
[8] A. Afkhami, F. Soltani-Felehgari, T. Madrakian, H. Ghaedi, Surface decoration of multi-walled carbon nanotubes modified carbon paste electrode with gold nanoparticles for electro-oxidation and sensitive determination of nitrite, Biosens. Bioelectron. 51 (2014) 379–385.
[9] C.H. Yang, T. Liu, S.H. Zhang, A novel nitrite amperometric sensor based on poly(L-cysteine) film electrode and its application in food analysis, Food Sci. 30 (2009) 158–161.
[10] L.P. Lu, S.Q. Wang, T.F. Kang, W.W. Xu, Synergetic effect of Pd-Fe nanoclusters: electrocatalysis of nitrite oxidation, Microchim. Acta 162 (2008) 81–85.
[11] Y. Zhang, S.L. Zhang, Z. Xiang, W. Ren, Y.C. Sun, S.L. Cai, Determination of nitrite by a nano-Au/melamine modified electrode, Chin. J. Anal. Lab. 32 (2013) 63–67.
[12] M.Y. Li, L.M. Kong, P.S. Zhu, B. Peng, S.S. Huang, Y.X. Yuan, Voltammetric determination of nitrite radical using the modified electrode L-cys/Au immobilized with cytochrome c, Phys. Test. Chem. Anal. B (Chem. Anal.) 44 (2008) 495–498.
[13] Z. He, R.V. Gudavarthy, J.A. Koza, J.A. Switzer, Room-temperature electrochemical reduction of epitaxial magnetite films to epitaxial iron films, J. Am. Chem. Soc. 133 (2011) 12358–12361.
[14] Y. Liu, J. Zhou, J. Gong, W.P. Wu, N. Bao, Z.Q. Pan, H.Y. Gu, The investigation of electrochemical properties for $Fe_3O_4$@Pt nanocomposites and an enhancement sensing for nitrite, Electrochim. Acta 111 (2013) 876–887.
[15] C.M. Yu, Y.D. Wang, L. Wang, Z.K. Zhu, N. Bao, H.Y. Gu, Nanostructured biosensors built with layer-by-layer electrostatic assembly of hemoglobin and $Fe_3O_4$@Pt nanoparticles, Colloids Surf., B 103 (2013) 231–237.
[16] C.M. Yu, J.W. Guo, H.Y. Gu, Electrocatalytical oxidation of nitrite and its determination based on Au@$Fe_3O_4$ nanoparticles, Electroanal 22 (2010) 1005–1011.
[17] H. Zhang, X. Zhong, J.J. Xu, H.Y. Chen, $Fe_3O_4$/polypyrrole/Au nanocomposites with core/shell/shell structure: synthesis, characterization, and their electrochemical properties, Langmuir 24 (2008) 13748–13752.
[18] G.N. Wang, X.J. Zhang, A. Skallberg, Y.X. Liu, Z.J. Hu, X.F. Mei, K. Uvdal, One-step synthesis of water-dispersible ultra-small $Fe_3O_4$ nanoparticles as contrast agents for T1 and T2 magnetic resonance imaging, Nanoscale 6 (2014) 2953–2963.
[19] G.S. Wang, G.Y. Chen, Z.Y. Wei, X.F. Dong, M. Qi, Multifunctional $Fe_3O_4$/graphene oxide nanocomposites for magnetic resonance imaging and drug delivery, Mater. Chem. Phys. 141 (2013) 997–1004.
[20] S.J. Hoseini, H. Nasrabadi, M. Azizi, A.S. Beni, R. Khalifeh, $Fe_3O_4$ nanoparticles as an efficient and magnetically recoverable catalyst for friedel–crafts acylation reaction in solvent-free conditions, Synth. Commun. 43 (2013) 1683–1691.
[21] X. Yang, F.B. Xiao, H.W. Lin, F. Wu, D.Z. Chen, Z.Y. Wu, A novel $H_2O_2$ biosensor based on $Fe_3O_4$–Au magnetic nanoparticles coated horseradish peroxidase and graphene sheets–Nafion film modified screen-printed carbon electrode, Electrochim. Acta 109 (2013) 750–755.
[22] X.C. Tan, J.L. Zhang, S.W. Tan, D.D. Zhao, Z.W. Huang, Y. Mi, Z.Y. Huang, Amperometric hydrogen peroxide biosensor based on horseradish peroxidase immobilized on $Fe_3O_4$/chitosan modified glassy carbon electrode, Electroanal 21 (2009) 1514–1520.
[23] H.P. Peng, R.P. Liang, L. Zhang, J.D. Qiu, Facile preparation of novel core–shell enzyme–Au–polydopamine–$Fe_3O_4$ magnetic bionanoparticles for glucose sensor, Biosens. Bioelectron. 42 (2013) 293–299.
[24] S. Srivastava, R. Awasthi, N.S. Gajbhiye, V. Agarwal, A. Singh, A. Yadav, R.K. Gupta, Innovative synthesis of citrate-coated superparamagnetic $Fe_3O_4$ nanoparticles and its preliminary applications, J. Colloid Interface Sci. 359 (2011) 104–111.
[25] C.J. Yu, C.Y. Lin, C.H. Liu, T.L. Cheng, W.L. Tseng, Synthesis of poly(diallyldimethylammonium chloride)-coated $Fe_3O_4$ nanoparticles for colorimetric sensing of glucose and selective extraction of thiol, Biosens. Bioelectron. 26 (2010) 913–917.